THE JOURNAL OF PHYSICAL CHEMISTRY LETTERS
A JOURNAL OF THE AMERICAN CHEMICAL SOCIETY

pubs.acs.org/JPCL

Letter

Picosecond Charge-Transfer-State Dynamics in Wide Band Gap Polymer–Non-Fullerene Small-Molecule Blend Films Investigated via Transient Infrared Spectroscopy

Matthias Nuber, Lukas V. Spanier, Sebastian Roth, Georgi N. Vayssilov, Reinhard Kienberger, Peter Müller-Buschbaum, and Hristo Iglev*

Cite This: J. Phys. Chem. Lett. 2022, 13, 10418–10423

Read Online

ABSTRACT: Organic solar cells based on wide band gap polymers and nonfullerene small-molecule acceptors have demonstrated remarkably good device performances. Nevertheless, a thorough understanding of the charge-transfer process in these materials has not been achieved yet. In this study, we use Fano resonance signals caused by the interaction of broad electronic charge carrier absorption and the molecular vibrations of the electron acceptor molecule to monitor the charge-transfer state dynamics. In our time-resolved infrared spectroscopy experiments, we find that in the small-molecule acceptor, they have additional dynamics on the order of a few picoseconds. A change in the solvent used in thin film deposition, leading to different morphologies, influences this time further. We interpret our findings as the dynamics of the charge-transfer state at the interface of the electron donor and the electron- acceptor. The additional mid-infrared transient signal is generated in this state, as both electron and hole polarons can interact with small-molecule acceptor vibrational modes.

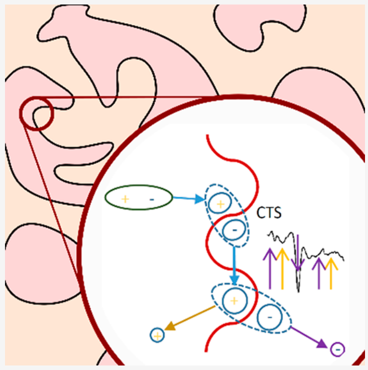

Organic semiconductors can be used in a wide range of optoelectronic applications. In particular, solution-processed bulk heterojunction (BHJ) organic solar cells (OSCs) have attained considerable attention due to their high possible conversion efficiencies.[1,2] The use of small-molecule nonfullerene acceptors, instead of fullerene molecules, enabled a better tuning of the optoelectronic properties of the electron acceptor to the electron donor and thereby improved the respective device performance.[3−5] In addition, a wider range of the solar spectrum can be captured by using wide band gap polymers and by tuning the band gaps of both materials accordingly.[6−8]

In all systems, the charge carriers created by the photo-excitation are usually described as bound excitons which then diffuse to the donor–acceptor interface.[9] At the interface, a charge-transfer state (CTS) is formed in which one of the charges transfers to an energetically favorable material.[9] Within these materials, charges interact with the respective structure and form polarons, in which the charges are Coulombically screened by a counteracting molecule rearrangement.[10,11] On organic semiconductors, polarons are known to exhibit very broad electronic absorptions that can be monitored in the mid-infrared spectrum.[12] An interaction between a polaronic charge and a vibrational mode in the respective material can lead to a particularly enhanced or suppressed signal close to the ground-state mode. These effects are often summarized as infrared activated vibrations (IRAVs).[12,13] While the exact interaction mechanism often remains unclear, they nevertheless can act as indicators for processes that involve a structural response of the material to a charge being present. Among the different explanations for IRAV signals, Fano resonances stand out, as they can lead to an antiresonance, which is a manifestly reduced signal at the original vibrational mode.[14] A Fano resonance occurs as an interaction between a broad (in this case the wide electronic polaron absorption) and a sharp signal (here, the well-defined vibrational mode).[15] In the literature, Fano resonances have been used in similar systems as a proxy to probe the charges' environment in a blend with the resonance only being present with the charge in proximity to the respective material.[16]

For the performance of an OSC, the CTS proves to be a critical stage for an efficient charge separation.[17,18] This process follows the diffusion of the exciton to the donor–acceptor interface, for which different time scales have been reported in the literature. While in some cases diffusion times in the picosecond range have been published, other studies found faster processes in the femtosecond regime,[19] in particular for intimately intermixed samples, in which little or no diffusion is necessary to reach the heterojunction.[20,21] As this time strongly depends on the domain size in the samples, a

Received: September 19, 2022
Accepted: October 28, 2022
Published: November 3, 2022

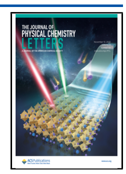

https://doi.org/10.1021/acs.jpclett.2c02864
J. Phys. Chem. Lett. 2022, 13, 10418−10423

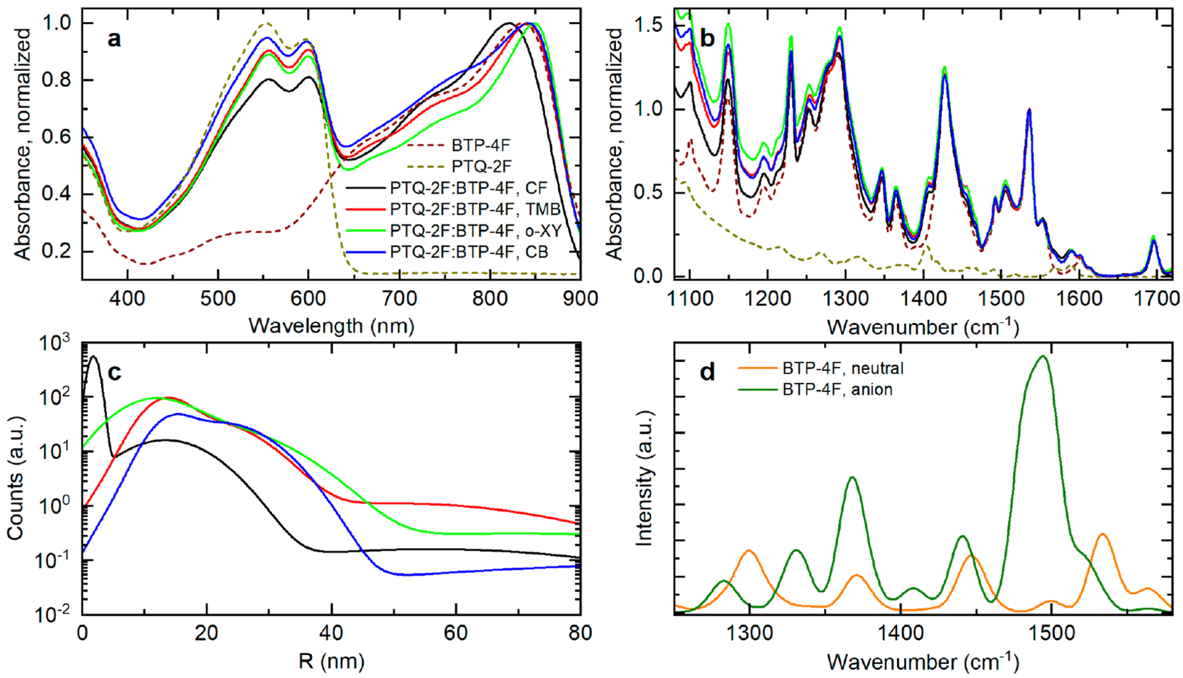

Figure 1. (a) UV-VIS spectra of PTQ-2F:BTP-4F blend films spin coated from different solvents (CF = chloroform, TMB = 1,2,4-trimethylbenzene, o-XY = ortho-xylene, CB = chlorobenzene) and neat BTP-4F and PTQ-2F films for comparison. All spectra are normalized to their maximum absorbance. (b) Infrared spectra of the samples, legend as in (a); all spectra are normalized to the mode at 1535 cm^{-1}. (c) Domain size distribution as obtained from GISAXS fits. (d) Calculated IR spectra for the neutral and anionic BTP-4F small-molecule acceptor.

direct comparison of this morphology-dependent process proves to be difficult. To examine the dynamics of the CTS and the electron/hole transfer, a wide range of pump−probe experiments have been used. In many cases, visible transient absorption (vis-TA) measurements have been interpreted with a delayed rise of the acceptor material signal after a hole or electron transfer.[10,22−25] Nevertheless, this assignment remains ambiguous concerning the exact dynamics of the CTS, which need to be considered separately from the mere transfer of an electron or a hole to its respective acceptor material.[26] The critical phase in the charge separation process should be considered longer, as the recombination probability remains enlarged until both charges separately diffuse away from the donor−acceptor interface.

In this article, we use picosecond vis-pump/mid-infrared-probe spectroscopy to investigate the dynamics of the CTS in a wide band gap polymer:nonfullerene small-molecule blend (PTQ-2F:BTP-4F) forming bulk heterojunctions. We select distinct Fano resonances to distinguish the CTS dynamics from broad polaronic states. In combination with DFT calculations, we find that multiple BTP-4F vibrational modes form strong antiresonance that probes polaronic charge carriers on or close to the BTP-4F phase. We show that the structure of the blend films, varied due to different solvents used in the blend film deposition, influences the CTS lifetime.

Recent combinations of donor−acceptor systems were tuned in a way that the visible absorptions of both donor and acceptor molecules are complementary, covering a wider spectral range. In this study, we select PTQ-2F (also called PTQ10 in the literature; full name in the Supporting Information (SI)) as a wide band gap electron donor polymer and the nonfullerene small-molecule acceptor BTP-4F (also called Y6 in the literature; full name in the SI). We use different solvents to tailor the structure of the blend films, thereby influencing the dynamics of the photovoltaic processes. The absorbance spectra of the blend films can be found in Figure 1a (see also Supporting Figure S1).

The broad absorption by both molecules is clearly visible, as the electron donor polymer PTQ-2F mainly absorbs from 500 to 650 nm and the electron acceptor molecule BTP-4F exhibits an absorbance spectrum in the red to near-infrared from 650 to 800 nm. A slight difference in the absorbance spectra of the isolated components compared to the bulk heterojunction is indicative of the successful formation of the interpenetrating network.[27] Investigating the morphology of the PTQ-2F:BTP-4F blend films using grazing incidence small-angle X-ray scattering (GISAXS),[28] we find that the choice of the solvent from which the samples are coated indeed influences the average PTQ-2F domain sizes (see Figure 1c and the related Supporting Figure S2). In particular, a strong difference in the polymer cluster sizes is observed between chloroform and the other used solvents, as the former exhibits an additional small size component. For analysis, we use horizontal line cuts of the 2D GISAXS data at the critical angle of PTQ-2F and model them using three cylindrical form factors. Regarding their infrared spectra (see Figure 1b and Supporting Figure S3), the small molecule acceptor BTP-4F proves to be dominant compared to the rather weak modes associated with the electron donor polymer PTQ-2F. In particular, a plethora of strong vibrational absorptions of BTP-4F can be found in the fingerprint region between 1100 and 1600 cm^{-1}. While a fundamental assignment of the modes proves to be very difficult, density functional (DFT) calculations help to associate the signals to specific regions and molecular bonds of the molecule. In this study, we use DFT with the PBE0 hybrid exchange-correlation functional as implemented in the ORCA program[29−31] to simulate the electronic structure and vibrational frequencies of the neutral BTP-4F molecule (see Figure 1d). To examine the effect of an additional charge on the BTP-4F molecule, the spectrum of a BTP-4F anion has

https://doi.org/10.1021/acs.jpclett.2c02864
J. Phys. Chem. Lett. 2022, 13, 10418−10423

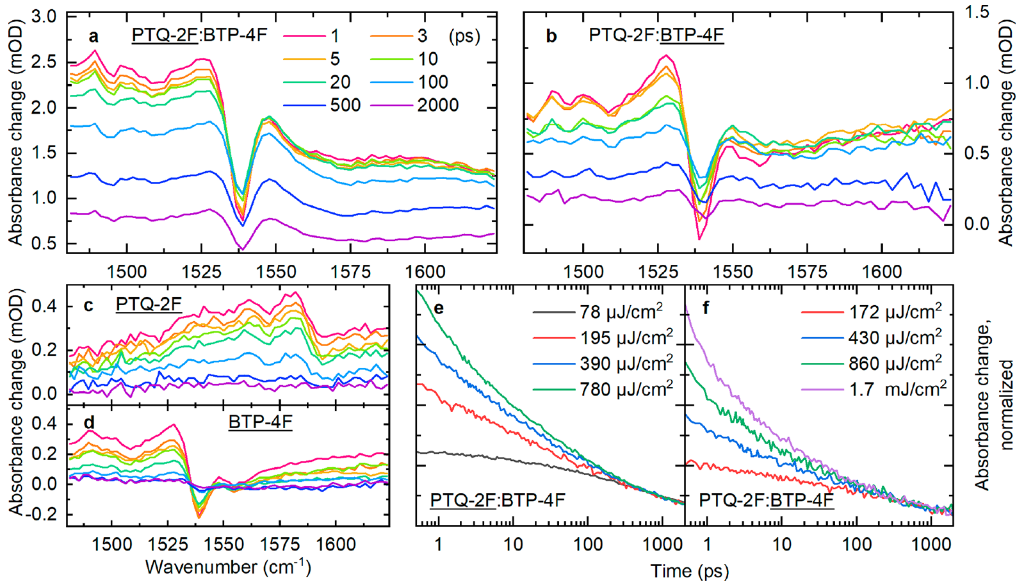

Figure 2. (a, b) Transient absorption spectra of PTQ-2F:BTF-4F blend films spin coated from CF, excited in the electron donor (a) and acceptor (b). (c, d) Transient absorption spectra of neat PTQ-2F (c) and BTP-4F (d) films. (e, f) Dynamics of the background signal at 1500 cm^{-1} of PTQ-2F:BTF-4F dissolved from CF, excited in the electron donor (e) and acceptor (f) normalized to their dynamics in the few hundreds ps region.

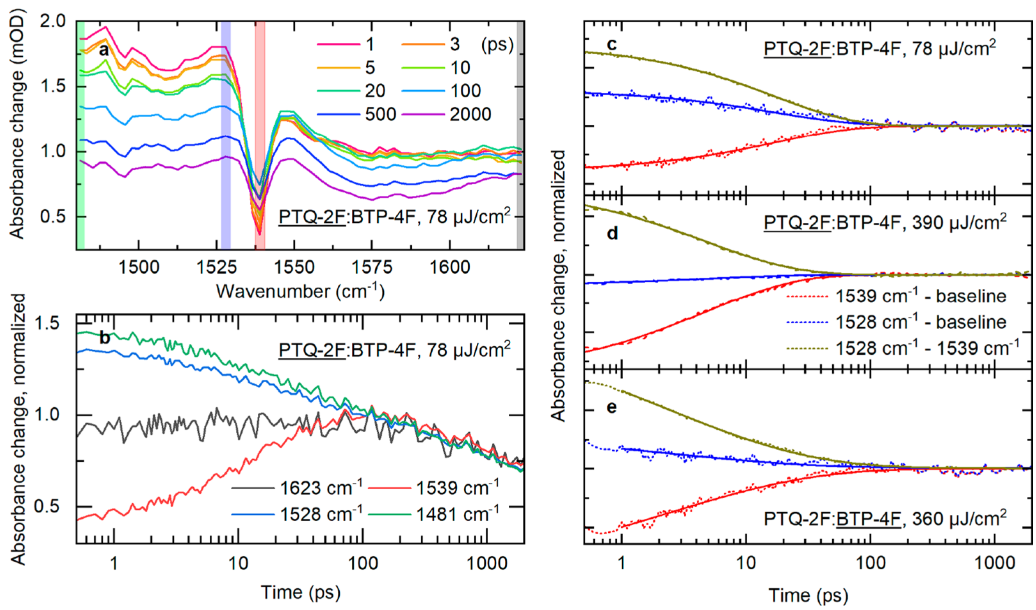

Figure 3. (a) Transient absorption spectra of PTQ-2F:BTF-4F blend films spin coated from TMB, excited in the electron donor. (b) Dynamics of selected pixel as marked in (a), normalized at 110 ps. (c−e) Additional dynamics of the Fano resonance for excitation in the electron donor (c, d) or electron acceptor (e) with different excitation densities. Stretched exponential fits (solid line, detailed fitting parameters in the SI) allow quantizing the charge-transfer state dynamics.

been calculated as well. For the anion, we find a strong additional mode, similar to an IRAV mode, close to the distinct ground-state absorption around 1535 cm^{-1} (see Figure 1d), which can be associated with collective vibration of the inden and malononitrile moieties dominated by the stretching C−C mode in the inden of the BTP-4F molecule. We further find that the additional charge in the anion is situated on this region of the small-molecule acceptor (see the charge density distribution in Supporting Figure S4). Therefore, we use this mode to investigate the interaction of polaronic charge carriers created upon photoexcitation and its interaction with the electron acceptor.

In our time-resolved mid-infrared spectroscopy measurements, we investigate that mode and the background signal in its vicinity.

We observe a broad background absorption emerging after excitation with an additional antiresonance around 1538 cm^{-1} (see Figure 2a and b). This general finding is independent of whether the electron donor (PTQ-2F) or the electron acceptor (BTP-4F) is resonantly excited. The broad infrared signal that by far exceeds the measurement region limited by the spectrometer-detector configuration can also be obtained measuring both active layer components isolated (see Figure 2c and d). We interpret this signal as of polaronic nature, similar to other broad mid-infrared absorptions reported in the

https://doi.org/10.1021/acs.jpclett.2c02864
J. Phys. Chem. Lett. 2022, 13, 10418−10423

literature for organic semiconductors (A more detailed discussion on the origin of the broad mIR transient background can be found in the SI).[32−34] With the excitation densities employed in our experiments (from a few tens to few hundreds of $\mu J/cm^{-2}$), we find that higher order effects, such as non-geminate bimolecular polaron recombination, dominate the dynamics in our samples for the first tens of ps (see Figure 2e and f). A comparison with the neat PTQ-2F and BTP-4F films (see Supporting Figures S5 and S6) reveals that the higher order effects appear to originate in the donor polymer PTQ-2F, as the neat small-molecule acceptor BTP-4F shows no changes in its tens of picoseconds dynamics with increasing excitation density. Although in the literature a considerable non-geminate recombination has been observed for BTP-4F, it highly depends on the thin film morphology.[35]

Therefore, our findings point toward a morphology-dependent difference of the charge mobilities in PTQ-2F and BTP-4F, suppressing the non-geminate recombination in BTP-4F in our experiments.

While the polaronic broadband absorption signal is rather unstructured, additional signals can be found. Their spectral shape at first glance resembles a bleaching signal of the infrared ground state modes. A closer comparison shows that the bleaching signal is slightly shifted in frequency and that the signal shape does not exactly mirror the original vibrational mode (see Supporting Figure S7). Thus, a broader range of possible interactions needs to be considered. As another interpretation, antiresonances need to be considered.

In the literature, antiresonances are usually associated with Fano resonance phenomena. They have been observed in a variety of organic semiconductor systems[14,33] or similar materials[36,37] and have also been used to track charge carriers within active layers.[16] In our experiments, we find Fano resonances due to the interaction of the broadband electronic absorption of polarons and the narrow vibrational states of the small-molecule acceptor, which arise within our time resolution of approximately 0.5 ps. We will later discuss how the specific bleaching-like signal very close to the ground-state absorption exhibits a different dynamic than the polaronic background. This behavior conflicts with an assignment as a simple ground-state bleaching and points toward an anti-resonance.

The Fano resonances can act as a probe for the charge carrier population on or close to the respective material.

Monitoring the dynamics of the Fano resonance reveals an additional process at early delay times. Normalizing the broad background signal and the Fano resonance at longer delay times (see Figure 3b) allows separation of the additional process visible around the Fano resonance from the polaronic dynamics. We find that the Fano resonance signal exhibits an additional dynamic on the order of a few to a few tens of picoseconds. This additional process can only be found in an active layer BHJ composition but not for the neat materials that also exhibit polaron formation[13,35] (see Supporting Figure S8). Therefore, we conclude that its physical origin lies within the charge-transfer process between the electron donor PTQ-2F and the electron acceptor molecule BTP-4F, which is only present in the BHJ geometry. We can exclude effects such as a polaron formation or stabilization process, akin to dynamics reported in perovskites,[38,39] that could be expected on a ps time scale due to the lack of a similar additional signal in the neat material (see Figure S8 in the SI). The same argument relating to the neat material also holds true for other effects such as a diffusion or hopping between acceptor molecules (a more detailed discussion can be found in the SI). We interpret our signal as due to the interaction of the broad electronic absorption of both hole and electron polaron in their respective acceptor molecule with the vibrational modes of the BTP-4F phase. As the occurrence of a Fano resonance requires a certain proximity of the polarons causing the broad electronic absorption and the BTP-4F molecules exhibiting the vibrational modes, the additional Fano dynamics appears to be an effect of the interaction between the hole polarons on the PTQ-2F polymer and BTP-4F molecules close to them. Considering the charge generation process as described in the literature, we conclude that the early dynamics visible in the antiresonance monitors the lifetime of the CTS. In this state, the excitonic initial excitations have already diffused to the phase boundary and a charge transfer has occurred. In the CTS, the charges are still Coulombically bound and, therefore, both polarons are still very close to the donor−acceptor interface. From this state, the charges can either recombine or separate to their respective acceptor material as free charge carriers.

The CTS proves to be of high relevance for the efficiency of OSCs. In the literature, a strong dependence on the morphology of the sample was reported.[40−44] Varying the solvent from which the blend films are spin coated leads to different sample morphologies of the BHJ structure as shown above. We find that the lifetime of the CTS, evaluated from stretched exponential fits as shown in Figure 3c−e, generally increases as the polymer clusters embedded in the BTP-4F phase grow in size (see Table 1). Without surprise, there is no simple one-to-one relation between domain sizes seen in GISAXS and CTS times. Reasons might be in the complex local morphology of the donor−acceptor interface or in the presence of a molecularly intermixed third phase between donor and acceptor. The trend shown in Table 1 is independent of whether the electron donor or the acceptor is excited.

Table 1. CTS Characteristic Time Constants as Obtained from a Stretched Exponential Fit and PTQ-2F Domain Sizes from GISAXS Data Analysis[a]

PTQ-2F:BTP-4F solvent	τ_{PTQ-2F}/ps	PTQ-2F 1st domain size/nm	PTQ-2F 2nd domain size/nm	PTQ-2F 3rd domain size/nm
chloroform	10.6 ± 0.7	1.7 ± 0.4	13 ± 1	55 ± 5
1,2,4-trimethylbenzene	16.9 ± 0.7	13 ± 1	20 ± 1	50 ± 5
orthoxylene	21.2 ± 0.9	11.0 ± 0.9	19 ± 1	68 ± 7
chlorobenzene	22.0 ± 2.6	14 ± 1	22 ± 2	104 ± 12

[a]The samples were excited with approximately 80 $\mu J/cm^2$ in the electron donor polymer PTQ-2F.

We additionally find a dependence of the characteristic times on the excitation density. With increasing excitation power, the characteristic CTS times decrease (see Figure 3c and d and Supporting Table S1) as the bimolecular component at early delay times becomes more dominant (see Figure 2e and f). From a principle point of view, the CTS recombines geminately and should, therefore, exhibit a lifetime independent of the excitation densities. Nevertheless, at the pump densities required for our experimental method, a non-geminate recombination path of the CTS interacting with

https://doi.org/10.1021/acs.jpclett.2c02864
J. Phys. Chem. Lett. 2022, 13, 10418−10423

either free charge carriers or excitons could be imagined as well. Thus, we associate this behavior with the recombination of the CTS due to another charge carrier being present in its vicinity as a result of the relatively high excitation density. Comparing the Fano resonance dynamics for a similar excitation density into both PTQ-2F and BTP-4F, we cannot resolve significant differences in the time constants obtained.

Therefore, we can conclude that the charge transfer occurs within our experimental time resolution. In the literature, that process has been reported with a variety of time constants, both experimentally[10,22,24,25] and theoretically.[45] The CTS observed in our study forms after the transfer of one of the charges and might not be distinguishable in transient absorption spectroscopy in other spectral regions.

In conclusion, using time-resolved mid-infrared spectroscopy, we investigate the charge carrier dynamics in PTQ-2F:BTP-4F donor−acceptor BHJ blend films with different morphologies. We measure broad polaronic absorptions with overlying Fano antiresonances due to the interaction with vibrational modes. Shortly after the optical excitation, these modes are particularly pronounced, with an additional dynamic at early delay times. These processes with characteristic times on the order of a few to tens of ps are associated with the CTS in which both hole and electron polarons can interact with the BTP-4F vibrational modes due to their proximity. We additionally find that the morphology of the BHJ structure strongly influences the CTS lifetime. Our results highlight the importance of the donor−acceptor interface and its properties for the charge carrier dynamics in the donor−acceptor BHJ. Combining time-resolved spectroscopy and structure characterization of donor−acceptor systems can help improve the performance of future OSC systems.

■ ASSOCIATED CONTENT

Supporting Information

The Supporting Information is available free of charge at https://pubs.acs.org/doi/10.1021/acs.jpclett.2c02864.

Experimental methods and sample preparation; details regarding DFT calculations. More detailed discussion of the mIR transient background origin. GISAXS line cuts, Fano resonance signal in neat BTP-4F, unscaled UV-VIS spectra and FTIR spectra of all samples. Fit parameters for stretched exponential fits at different excitation densities and for excitation into both electron donor and acceptor. (PDF)

Transparent Peer Review report available (PDF)

■ AUTHOR INFORMATION

Corresponding Author

Hristo Iglev − *Lehrstuhl für Laser- und Röntgenphysik, Physik-Department, Technische Universität München, 85748 Garching, Germany;* orcid.org/0000-0001-9208-0068; Email: hristo.iglev@ph.tum.de

Authors

Matthias Nuber − *Lehrstuhl für Laser- und Röntgenphysik, Physik-Department, Technische Universität München, 85748 Garching, Germany;* orcid.org/0000-0002-4409-3590

Lukas V. Spanier − *Lehrstuhl für Funktionelle Materialien, Physik-Department, Technische Universität München, 85748 Garching, Germany*

Sebastian Roth − *Lehrstuhl für Laser- und Röntgenphysik, Physik-Department, Technische Universität München, 85748 Garching, Germany*

Georgi N. Vayssilov − *Faculty of Chemistry and Pharmacy, University of Sofia, 1126 Sofia, Bulgaria;* orcid.org/0000-0002-5185-8002

Reinhard Kienberger − *Lehrstuhl für Laser- und Röntgenphysik, Physik-Department, Technische Universität München, 85748 Garching, Germany*

Peter Müller-Buschbaum − *Lehrstuhl für Funktionelle Materialien, Physik-Department, Technische Universität München, 85748 Garching, Germany; Heinz Maier-Leibnitz Zentrum (MLZ), Technische Universität München, 85748 Garching, Germany;* orcid.org/0000-0002-9566-6088

Complete contact information is available at: https://pubs.acs.org/10.1021/acs.jpclett.2c02864

Notes

The authors declare no competing financial interest.

■ ACKNOWLEDGMENTS

This research was supported by the Deutsche Forschungsgemeinschaft (DFG) via the Cluster of Excellence "e-conversion" (EXC 2089/1-390776260). M.N. thanks the "Studienstiftung des deutschen Volkes" for a Ph.D. scholarship. G.N.V. acknowledges the support by the project EXTREME, funded by the Bulgarian Ministry of Education and Science (D01-76/30.03.2021). P.M.-B. acknowledges funding by TUM.solar in the context of the Bavarian Collaborative Research Project Solar Technologies Go Hybrid (SolTech). We thank M. Schwartzkopf and S. V. Roth from DESY for their support with the installation of the GISAXS setup.

■ REFERENCES

(1) Zhang, M.; Zhu, L.; Zhou, G.; Hao, T.; Qiu, C.; Zhao, Z.; Hu, Q.; Larson, B. W.; Zhu, H.; Ma, Z.; et al. Single-Layered Organic Photovoltaics with Double Cascading Charge Transport Pathways: 18% Efficiencies. *Nat. Commun.* **2021**, *12*, 309.

(2) Zhan, L.; Li, S.; Xia, X.; Li, Y.; Lu, X.; Zuo, L.; Shi, M.; Chen, H. Layer-by-Layer Processed Ternary Organic Photovoltaics with Efficiency over 18. *Adv. Mater.* **2021**, *33*, e2007231.

(3) Li, S.; Liu, W.; Li, C.-Z.; Shi, M.; Chen, H. Efficient Organic Solar Cells with Non-Fullerene Acceptors. *Small* **2017**, *13*, 1701120.

(4) Nielsen, C. B.; Holliday, S.; Chen, H.-Y.; Cryer, S. J.; McCulloch, I. Non-Fullerene Electron Acceptors for Use in Organic Solar Cells. *Acc. Chem. Res.* **2015**, *48*, 2803−2812.

(5) Hou, J.; Inganäs, O.; Friend, R. H.; Gao, F. Organic Solar Cells Based on Non-Fullerene Acceptors. *Nat. Mater.* **2018**, *17*, 119−128.

(6) Jia, Z.; Qin, S.; Meng, L.; Ma, Q.; Angunawela, I.; Zhang, J.; Li, X.; He, Y.; Lai, W.; Li, N.; et al. High Performance Tandem Organic Solar Cells via a Strongly Infrared-Absorbing Narrow Bandgap Acceptor. *Nat. Commun.* **2021**, *12*, 178.

(7) Wang, K.; Lv, J.; Duan, T.; Li, Z.; Yang, Q.; Fu, J.; Meng, W.; Xu, T.; Xiao, Z.; Kan, Z.; et al. Simple Near-Infrared Nonfullerene Acceptors Enable Organic Solar Cells with 9% Efficiency. *ACS Appl. Mater. Interfaces* **2019**, *11*, 6717−6723.

(8) Gao, W.; Liu, T.; Ming, R.; Luo, Z.; Wu, K.; Zhang, L.; Xin, J.; Xie, D.; Zhang, G.; Ma, W.; et al. Near-Infrared Small Molecule Acceptor Enabled High-Performance Nonfullerene Polymer Solar Cells with over 13% Efficiency. *Adv. Funct. Mater.* **2018**, *28*, 1803128.

(9) Clarke, T. M.; Durrant, J. R. Charge Photogeneration in Organic Solar Cells. *Chem. Rev.* **2010**, *110*, 6736−6767.

(10) Wang, R.; Zhang, C.; Li, Q.; Zhang, Z.; Wang, X.; Xiao, M. Charge Separation from an Intra-Moiety Intermediate State in the

High-Performance PM6:Y6 Organic Photovoltaic Blend. *J. Am. Chem. Soc.* **2020**, *142*, 12751−12759.
(11) Sudakov, I.; van Landeghem, M.; Lenaerts, R.; Maes, W.; van Doorslaer, S.; Goovaerts, E. The Interplay of Stability Between Donor and Acceptor Materials in a Fullerene-Free Bulk Heterojunction Solar Cell Blend. *Adv. Energy Mater.* **2020**, *10*, 2002095.
(12) Kahmann, S.; Fazzi, D.; Matt, G. J.; Thiel, W.; Loi, M. A.; Brabec, C. J. Polarons in Narrow Band Gap Polymers Probed over the Entire Infrared Range: A Joint Experimental and Theoretical Investigation. *J. Phys. Chem. Lett.* **2016**, *7*, 4438−4444.
(13) Stallhofer, K.; Nuber, M.; Kienberger, R.; Körstgens, V.; Müller-Buschbaum, P.; Iglev, H. Dynamics of Short-Lived Polaron Pairs and Polarons in Polythiophene Derivatives Observed via Infrared-Activated Vibrations. *J. Phys. Chem. C* **2019**, *123*, 28100−28105.
(14) Horovitz, B.; Österbacka, R.; Vardeny, Z. V. Multiple Fano Effect in Charge Density Wave Systems. *Synth. Met.* **2004**, *141*, 179−183.
(15) Fano, U. Effects of Configuration Interaction on Intensities and Phase Shifts. *Phys. Rev.* **1961**, *124*, 1866−1878.
(16) Kahmann, S.; Salazar Rios, J. M.; Zink, M.; Allard, S.; Scherf, U.; Dos Santos, M. C.; Brabec, C. J.; Loi, M. A. Excited-State Interaction of Semiconducting Single-Walled Carbon Nanotubes with Their Wrapping Polymers. *J. Phys. Chem. Lett.* **2017**, *8*, 5666−5672.
(17) Coropceanu, V.; Chen, X.-K.; Wang, T.; Zheng, Z.; Brédas, J.-L. Charge-Transfer Electronic States in Organic Solar Cells. *Nat. Rev. Mater.* **2019**, *4*, 689−707.
(18) Dimitrov, S. D.; Azzouzi, M.; Wu, J.; Yao, J.; Dong, Y.; Tuladhar, P. S.; Schroeder, B. C.; Bittner, E. R.; McCulloch, I.; Nelson, J.; et al. Spectroscopic Investigation of the Effect of Microstructure and Energetic Offset on the Nature of Interfacial Charge Transfer States in Polymer: Fullerene Blends. *J. Am. Chem. Soc.* **2019**, *141*, 4634−4643.
(19) Bolzonello, L.; Bernal-Texca, F.; Gerling, L. G.; Ockova, J.; Collini, E.; Martorell, J.; van Hulst, N. F. Photocurrent-Detected 2D Electronic Spectroscopy Reveals Ultrafast Hole Transfer in Operating PM6/Y6 Organic Solar Cells. *J. Phys. Chem. Lett.* **2021**, *12*, 3983−3988.
(20) Scarongella, M.; de Jonghe-Risse, J.; Buchaca-Domingo, E.; Causa', M.; Fei, Z.; Heeney, M.; Moser, J.-E.; Stingelin, N.; Banerji, N. A Close Look at Charge Generation in Polymer:Fullerene Blends with Microstructure Control. *J. Am. Chem. Soc.* **2015**, *137*, 2908−2918.
(21) Paraecattil, A. A.; Banerji, N. Charge Separation Pathways in a Highly Efficient Polymer: Fullerene Solar Cell Material. *J. Am. Chem. Soc.* **2014**, *136*, 1472−1482.
(22) Sun, C.; Pan, F.; Chen, S.; Wang, R.; Sun, R.; Shang, Z.; Qiu, B.; Min, J.; Lv, M.; Meng, L.; et al. Achieving Fast Charge Separation and Low Nonradiative Recombination Loss by Rational Fluorination for High-Efficiency Polymer Solar Cells. *Adv. Mater.* **2019**, *31*, e1905480.
(23) Wang, R.; Xu, J.; Fu, L.; Zhang, C.; Li, Q.; Yao, J.; Li, X.; Sun, C.; Zhang, Z.-G.; Wang, X.; et al. Nonradiative Triplet Loss Suppressed in Organic Photovoltaic Blends with Fluoridated Nonfullerene Acceptors. *J. Am. Chem. Soc.* **2021**, *143*, 4359−4366.
(24) Wu, J.; Lee, J.; Chin, Y.-C.; Yao, H.; Cha, H.; Luke, J.; Hou, J.; Kim, J.-S.; Durrant, J. R. Exceptionally Low Charge Trapping Enables Highly Efficient Organic Bulk Heterojunction Solar Cells. *Energy Environ. Sci.* **2020**, *13*, 2422−2430.
(25) Zhou, G.; Zhang, M.; Chen, Z.; Zhang, J.; Zhan, L.; Li, S.; Zhu, L.; Wang, Z.; Zhu, X.; Chen, H.; et al. Marcus Hole Transfer Governs Charge Generation and Device Operation in Nonfullerene Organic Solar Cells. *ACS Energy Lett.* **2021**, *6*, 2971−2981.
(26) Vandewal, K. Interfacial Charge Transfer States in Condensed Phase Systems. *Annu. Rev. Phys. Chem.* **2016**, *67*, 113−133.
(27) Yang, X.; Loos, J.; Veenstra, S. C.; Verhees, W. J. H.; Wienk, M. M.; Kroon, J. M.; Michels, M. A. J.; Janssen, R. A. J. Nanoscale Morphology of High-Performance Polymer Solar Cells. *Nano Lett.* **2005**, *5*, 579−583.
(28) Müller-Buschbaum, P. The Active Layer Morphology of Organic Solar Cells Probed with Grazing Incidence Scattering Techniques. *Adv. Mater.* **2014**, *26*, 7692−7709.
(29) Neese, F. The ORCA Program System. *WIREs Comput. Mol. Sci.* **2012**, *2*, 73−78.
(30) Neese, F. Software Update: The ORCA Program System, Version 4.0. *WIREs Comput. Mol. Sci.* **2018**, *8*, e1327 DOI: 10.1002/wcms.1327.
(31) Perdew; Burke; Ernzerhof. Generalized Gradient Approximation Made Simple. *Phys. Rev. Lett.* **1996**, *77*, 3865−3868.
(32) Pensack, R. D.; Asbury, J. B. Ultrafast Probes of Charge Transfer States in Organic Photovoltaic Materials. *Chem. Phys. Lett.* **2011**, *515*, 197−205.
(33) Österbacka, R.; Jiang, X. M.; An, C. P.; Horovitz, B.; Vardeny, Z. V. Photoinduced Quantum Interference Antiresonances in Pi-Conjugated Polymers. *Phys. Rev. Lett.* **2002**, *88*, 226401.
(34) Jeong, K. S.; Pensack, R. D.; Asbury, J. B. Vibrational Spectroscopy of Electronic Processes in Emerging Photovoltaic Materials. *Acc. Chem. Res.* **2013**, *46*, 1538−1547.
(35) Zhou, G.; Zhang, M.; Xu, J.; Yang, Y.; Hao, T.; Zhu, L.; Zhou, L.; Zhu, H.; Zou, Y.; Wei, G.; et al. Spontaneous Carrier Generation and Low Recombination in High-Efficiency Non-Fullerene Solar Cells. *Energy Environ. Sci.* **2022**, *15*, 3483−3493.
(36) Lapointe, F.; Rousseau, B.; Aymong, V.; Nguyen, M.; Biron, M.; Gaufrès, E.; Choubak, S.; Han, Z.; Bouchiat, V.; Desjardins, P.; et al. Antiresonances in the Mid-Infrared Vibrational Spectrum of Functionalized Graphene. *J. Phys. Chem. C* **2017**, *121*, 9053−9062.
(37) Eckstein, K. H.; Hirsch, F.; Martel, R.; Hertel, T. Infrared Study of Charge Carrier Confinement in Doped (6,5) Carbon Nanotubes. *J. Phys. Chem. C* **2021**, *125*, 5700−5707.
(38) Stallhofer, K.; Nuber, M.; Cortecchia, D.; Bruno, A.; Kienberger, R.; Deschler, F.; Soci, C.; Iglev, H. Picosecond Charge Localization Dynamics in CH3NH3PbI3 Perovskite Probed by Infrared-Activated Vibrations. *J. Phys. Chem. Lett.* **2021**, *12*, 4428−4433.
(39) Guzelturk, B.; Winkler, T.; van de Goor, T. W. J.; Smith, M. D.; Bourelle, S. A.; Feldmann, S.; Trigo, M.; Teitelbaum, S. W.; Steinrück, H.-G.; La Pena, G. A. de; et al. Visualization of Dynamic Polaronic Strain Fields in Hybrid Lead Halide Perovskites. *Nat. Mater.* **2021**, *20*, 618−623.
(40) Karki, A.; Vollbrecht, J.; Gillett, A. J.; Xiao, S. S.; Yang, Y.; Peng, Z.; Schopp, N.; Dixon, A. L.; Yoon, S.; Schrock, M.; et al. The Role of Bulk and Interfacial Morphology in Charge Generation, Recombination, and Extraction in Non-Fullerene Acceptor Organic Solar Cells. *Energy Environ. Sci.* **2020**, *13*, 3679−3692.
(41) Lin, Y. L.; Fusella, M. A.; Rand, B. P. The Impact of Local Morphology on Organic Donor/Acceptor Charge Transfer States. *Adv. Energy Mater.* **2018**, *8*, 1702816.
(42) Zhu, W.; Spencer, A. P.; Mukherjee, S.; Alzola, J. M.; Sangwan, V. K.; Amsterdam, S. H.; Swick, S. M.; Jones, L. O.; Heiber, M. C.; Herzing, A. A.; et al. Crystallography, Morphology, Electronic Structure, and Transport in Non-Fullerene/Non-Indacenodithienothiophene Polymer:Y6 Solar Cells. *J. Am. Chem. Soc.* **2020**, *142*, 14532−14547.
(43) Fukuhara, T.; Yamazaki, K.; Hidani, T.; Saito, M.; Tamai, Y.; Osaka, I.; Ohkita, H. Molecular Understanding of How the Interfacial Structure Impacts the Open-Circuit Voltage of Highly Crystalline Polymer Solar Cells. *ACS Appl. Mater. Interfaces* **2021**, *13*, 34357−34366.
(44) Dela Peña, T. A.; Khan, J. I.; Chaturvedi, N.; Ma, R.; Xing, Z.; Gorenflot, J.; Sharma, A.; Ng, F. L.; Baran, D.; Yan, H.; et al. Understanding the Charge Transfer State and Energy Loss Trade-Offs in Non-Fullerene-Based Organic Solar Cells. *ACS Energy Lett.* **2021**, *6*, 3408−3416.
(45) Dorfner, M. F. X.; Hutsch, S.; Borrelli, R.; Gelin, M. F.; Ortmann, F. Ultrafast Carrier Dynamics at Organic Donor−acceptor Interfaces—A Quantum-Based Assessment of the Hopping Model. *J. Phys. Mater.* **2022**, *5*, 024001.